Supplemental Material
for
"Rheology of Active Polymer-Like *T. Tubifex* Worms"

A. Deblais,[1] S. Woutersen,[2] and D. Bonn[1]

[1] *Van der Waals-Zeeman Institute, Institute of Physics, University of Amsterdam, 1098XH Amsterdam, The Netherlands.*
[2] *Van't Hoff Institute for Molecular Sciences, University of Amsterdam, Science Park 904, 1098XH Amsterdam, The Netherlands.*

This document provides supporting information to accompany the main text. Part I provides more information about the system studied in the paper, the active polymer-like *T. Tubifex* worm. It gives details on the procedure used to extract the size distribution, diffusion motion and microscopic characteristic time scale τ_{worm} describing the individual worm dynamics. Part II provides more details on the custom-designed rheology cell used to study the flow behaviour of an ensemble of active polymer-like worms in solution.

I. *Tubifex tubifex* worms

All batches of *T. Tubifex* worms studied in this paper were purchased from Aquarium Holgen, Jacob van Lennepstraat 64, 1053 HL Amsterdam, The Netherlands. To our knowledge, the origin of the worms can be either Poland, the UK or Belgium. They were extracted from their natural environment and kept in an aquarium for one week in order to be rinsed from any trace of pollutant, sludge or their own waste. We collected them after this step. The length of the worms can vary widely depending on the season, age, etc. while their width $W = 0.2 - 0.4\ mm$ remains almost constant [1].

1. *Size distribution*

The characteristic length L of the worms was determined by taking pictures (Nikon D5300 equipped with a macro-lens Sigma 105mm 1:2.8) of a low-concentration dispersion (so that individual worms can be distinguished from another) in a quasi-2D aquarium (see Suppl.Fig. 1a); a thin layer of water of 5 mm in height constrains the worms to move in quasi two dimensions. The whole setup was mounted on a LED panel providing a uniform light background. To control the temperature of the living medium (tap water), a transparent thermo-controlled cell was assembled underneath the aquarium. The water flow and its temperature were ensured via a temperature bath (Thermo Scientific, HAAKE A 25) connected to the cell.

A home-made routine developed in Matlab allowed us to accurately detect the shape of the worms, following the following protocol:
(i) The original image was converted in a 8-bit grey level [0-255] (an example is shown in Suppl.Fig. 3b,i);
(ii) A threshold was applied to differentiate the active polymer-like filament from the remaining background. Grey levels exceeding the threshold were assigned a value of 1 (black), the remaining levels a value of 0 (white) (Suppl.Fig. 3b,ii);
(iii) The resulting cluster of pixels covering the worm's shape was finally thinned to a 1-pixel-wide line using a skeletonization routine that erodes pixels by iteration. The (eventual) residual neighbourless pixels were elimi-

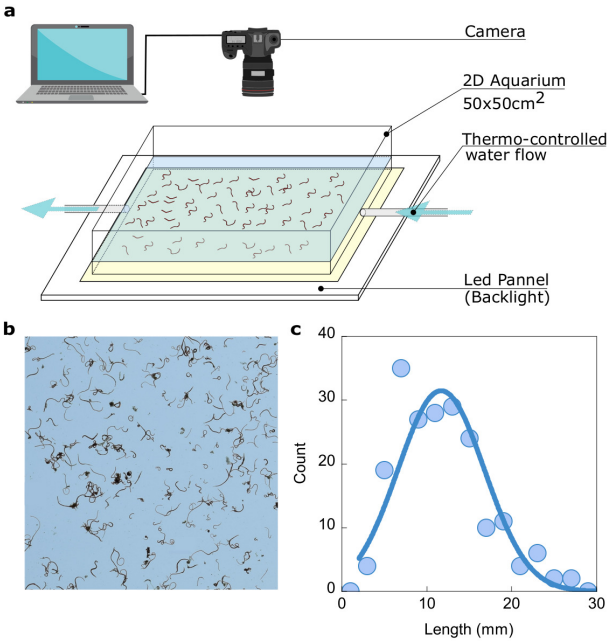

SUPPL. FIG. 1. | **Determination of the size distribution.**
a Sketch of the experimental setup used to determine the distribution length of the worms (not to scale) and to track the dynamics of the worms. A camera is taking picture of the collection of the living *T. Tubifex* worms dispersed in a thin layer of tap water at a controlled temperature T.
b Typical top-view picture used to determine the length of the worms. The picture size is 10×10 cm^2.
c Size distribution of the worm population. The continuous line is a Gaussian fit to the experimental data.

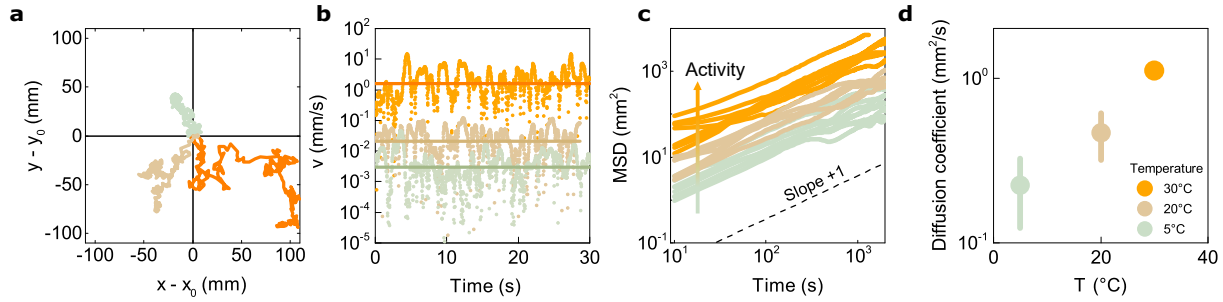

SUPPL. FIG. 2. | **Determination of the *T. Tubifex* velocity and diffusion coefficient.**
a The experimental setup described in Suppl.Fig. 1a was used to track the trajectory of a single worm as a function of time at a controlled temperature T. The solid traces of different colours are three examples of centre-of-mass trajectories of one-hour duration for the same *T. Tubifex* worm at three different temperatures $T = 5, 20, 30°\mathrm{C}$. The origin of the trajectories is set to $(x_0, y_0) = (0, 0)$.
b Instantaneous velocity of a single worm as function of temperature. The solid line is the averaged velocity $\langle v_{worm} \rangle$ extracted from the experimental data.
c Mean square displacement as a function of time MSD(t) of the same ten worms in water at $T = 5, 20, 30°\mathrm{C}$. The dashed line of slope 1 shows the expected scaling for a Brownian motion.
d Diffusion coefficient extracted from the MSD(t) as a function of temperature. Each measurement is an average over 10 trajectories of the same worm. The error bars (standard deviation) indicate the variability in the data.

nated using a simple algorithm to exclude non-connected pixels (Suppl.Fig. 3b,iii).

In this way we determined the length L of each of the worms of the batch under study. The averaged length of a typical batch studied in this paper was found to be L=11.7 mm with a standard deviation of 5 mm (Suppl.Fig. 1b).

2. *Velocity and Diffusion motion*

The *T. tubifex* worms are active swimmers; they are able to effectively move by contracting their segments. The thermal random motion of these worms is negligible compared to their active motion.

We characterized their instantaneous velocity and diffusive motion by using the thermo-controlled setup described in section I.1. We recorded movies at 0.1 frames per second for a duration of 1 hour to track the trajectory of an active polymer-like worm at a given temperature.

In Suppl.Fig. 2a, a single worm is tracked at three different temperatures $T = 5, 20, 30°\mathrm{C}$ from which we extracted the instantaneous velocity v_{worm} showed in Suppl.Fig. 2b. The temperature affects the averaged velocity $\langle v_{worm} \rangle$ of the *T. Tubifex* worm from ~ 5 μm s^{-1} at low activity (T=5° C) to ∼mm s^{-1} at high level of activity (T=30° C).

We also characterized their diffusion dynamics at longer time scales. The outcomes clearly show that the higher the temperature, the bigger the area explored by the worm. This was confirmed by extracting the mean square displacement (MSD) as a function of time of such trajectories (Suppl.Fig. 2c). We measured the MSD for 10 worms at 3 different temperatures and extracted the averaged diffusion coefficient from the MSD. The results are showed in Suppl.Fig. 2d and confirm that the diffusion coefficient increases as the temperature of the system is increased. The error bars denote the variability on the extracted diffusion coefficient; this is due to the large polydispersity of the system (Suppl.Fig. 1): the larger the worm, the higher its diffusion coefficient.

3. *Microscopic time scale* τ_{worm}

An other dynamical feature of these worms is their ability to oscillate, referred to here as 'wiggling' movement (Suppl.Fig. 3a). Similarly to is done for normal polymers undergoing thermal fluctuations, we describe the activity of the worms as their ability to wiggle in time, and quantify the time scale of their shape fluctuations as a function of the level of activity. To do so, as described in the main text, we looked at the individual dynamics of *T. Tubifex* by taking image sequences at a frame rate of 50 frames per second using the setup described before (Suppl.Fig. 1a). We quantified the time-dependant variations in an active polymer-like worm's end-to-end distance $\delta r_e(t) = r_e(t) - \langle r_e \rangle_t$ by tracking in time the two tips of the worm $r_e(t)$.

We automated the detection and tracking of the tips using a homemade routine which consists of the image processing steps described above in Sec. I.1; this allowed us to detect the two tips of the 1-pixel-wide segment and consequently track the end-to-end distance $r_e(t)$ in time of the worm as showed in Suppl.Fig. 3b,iv-v. At higher level of activities the worm can have complex spatial conformations, make knots and entangling itself; this makes the detection of the tip impossible and we lost in such cases the worm traces in few time steps. Such loss of

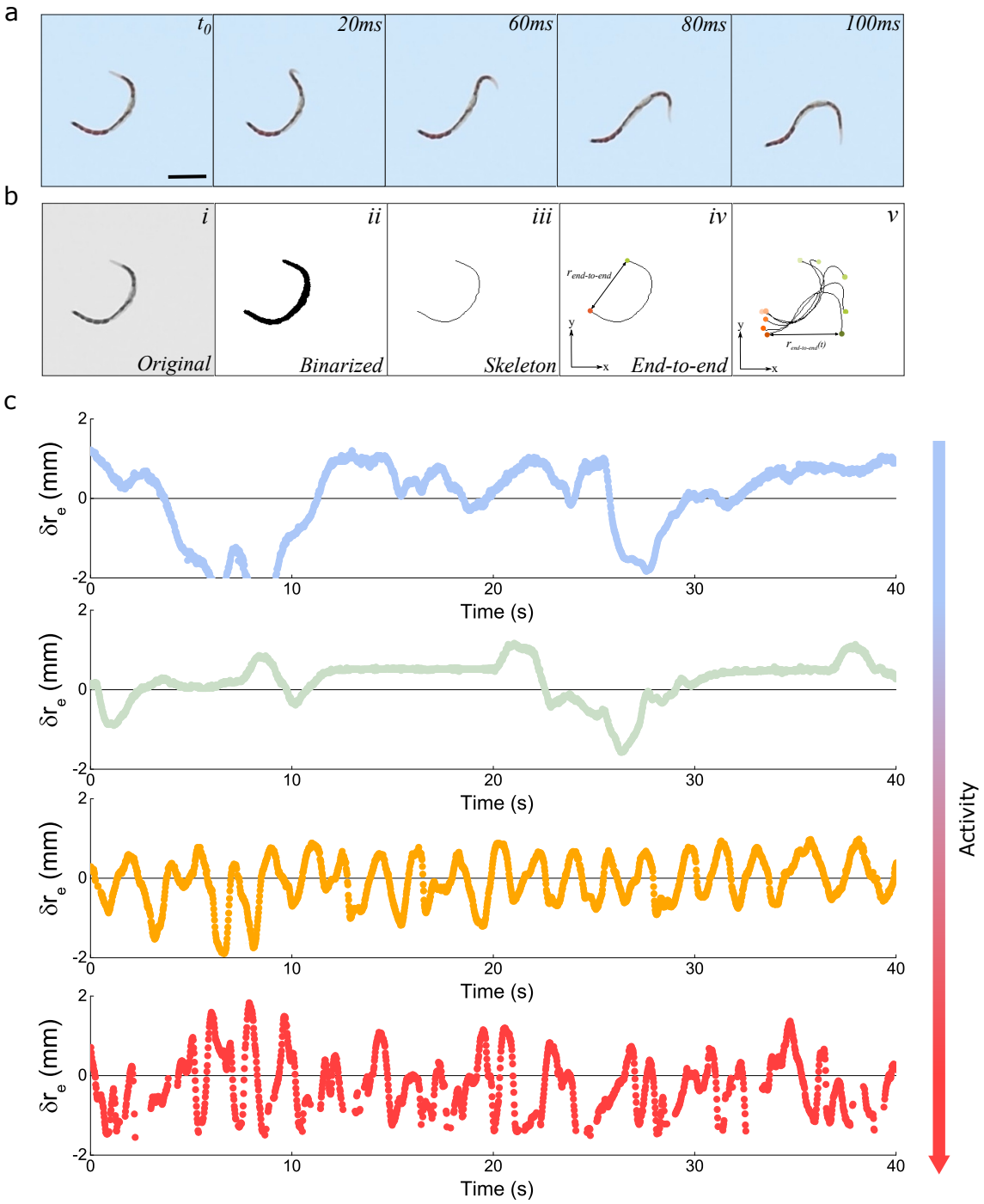

SUPPL. FIG. 3. | **Tracking the microscopic dynamics of a single *T. Tubifex* worm.**
a Sequence of pictures of a single worm in water at $T = 20°C$, initially recorded at a frame rate of 50 frames per second. The scale bar represents 5 mm.
b Example of the image processing stages of the localization algorithm applied to a worm constrained to move in a quasi-two-dimensional thermo-controlled aquarium. (i) Unprocessed image, followed by thresholding (ii), and skeletonization (iii). The home-made algorithm allows us to accurately follow the end-to-end distance r_e (iv) of the active polymer in time (v).
c Fluctuation of the end-to-end distance $\delta(r)_e$ with respect to its averaged value as a function of time with addition of 5% of alcohol (blue, top), and for 3 different temperatures $T = 5, 20, 30°C$ (green to orange, bottom). The corresponding autocorrelation function is reported in Fig. 2 of the main text.

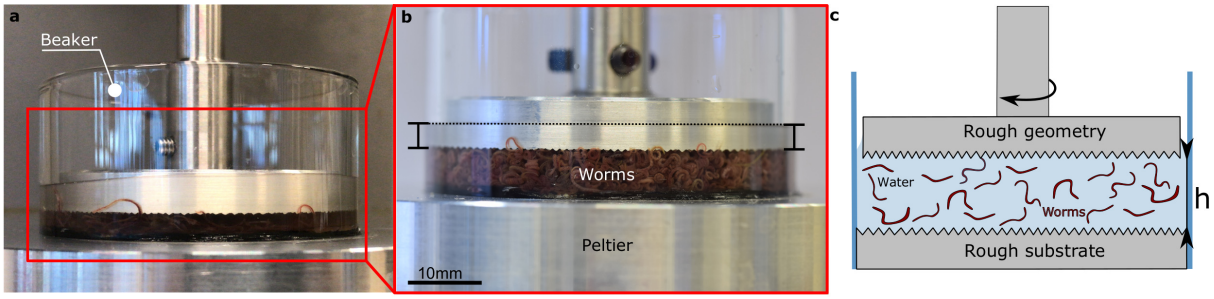

SUPPL. FIG. 4. | **Custom-designed geometry for rheology experiments.**
a,b Pictures of the custom-designed rheometry setup used to measure the rheology of the active polymer-like solutions. The side of the cell is made of a transparent glass 'beaker' and allows to visually confirm that the flow is homogeneous over the rotational sequence of measurement. The beaker is mounted on a Peltier cell to control the *in-situ* temperature T and thus control the level of activity of the worms. The gap geometry is set as the water level is anchored at half of the height of the upper geometry, as indicated by the H-symbol in the picture.
c Sketch of the geometry (not to scale) showing the characteristic lengths and the pyramidal shapes of the surface geometries.

tracking points is for example visible in the trace of $\delta r_e(t)$ in Suppl.Fig. 3c at $T = 30°$C (orange). The traces of the fluctuations of the end-to-end distances $\delta r_e(t)$ as function of the activity level (tuned via the temperature -green to orange- or by adding alcohol -blue-) are shown in the Suppl.Fig. 3. They clearly reveal the effect of activity on worm fluctuations: the higher the activity, the more temporal fluctuation are observed.

We further characterized these fluctuations by calculating the corresponding autocorrelation functions $g(t) = \frac{\langle \delta r_e(t) \delta r_e(t+\tau) \rangle_t}{\langle \delta r_e(t)^2 \rangle_t}$ and extracting the microscopic characteristic time τ_{worm} from the half-decay of $g(t)$ as shown in Fig. 2c in the main text.

II. Rheology

1. *Protocol*

The shear rheology of the living polymer-like worms was determined by rheology experiments in a custom-designed plate-plate geometry (See Suppl.Fig.4) adapted from a commercial rheometer (Anton Paar MCR 302). By inserting an equally rough top plate that just fits into the beaker, we created a plate-plate geometry in which the living polymers are confined and rheology experiments can be performed.

The roughness of the top and bottom plates is on the order of the diameter of the worms and allows us to control the velocity profile. The glass of the beaker is transparent, allowing us to visually confirm that the flows are homogeneous and to check the velocity profile under the geometry for a given shear rate (see Supplemental Video 1 and Section II.2 on velocity profiles).

The surfaces of the top and bottom plates (diameter R=25 mm) were patterned with pyramidal shapes (see Supplemental Figure 2) of 1 mm width and height. The gap of the geometry h is set as the water top level has to be anchored on the half-height of the upper geometry (see Suppl.Fig.2b). We performed the rheology measurements of the different active polymer-like solutions with a maximum shear rate of $10s^1$ to prevent harm to the worms. Measurement time per point was 6 s. All shear measurements were carried out twice to assure reproducibility, and show good agreement in all cases. The total time of the measurement run was constrained to two minutes in water to avoid inhomogeneity of the active system that sets in at longer time due to their diffusing motion (Suppl.Fig. 2) and spontaneous aggregation for biological reasons [2]. The rheology cell was preliminary calibrated during different Newtonian oil of known viscosity and the final shear viscosity was corrected accordingly.

2. *Velocity profiles*

We checked the possible effect of slip under the geometry by performing particle image velocimetry (PIV) measurements for 3 different values of the shear rate $\dot{\gamma} = 0.05, 0.1$ & $0.5s^{-1}$. The experiments were performed for a constant concentration of living worms of $\phi = 0.60$ and a constant gap $h = 5.85$ mm. Suppl.Fig. 5a shows a sketch of the experimental setup used to record determine the velocity profile from PIV measurements. In this experiment, ceramic hollow spheres of diameter 100 μm coated with silver (from LaVision company) are seeded in the living-worms solution. We used collimated light (Navitar) and a fast camera (Phantom V701) to visualize the particles in reflection, as shown in Suppl.Fig. 5b. The PIV is achieved by combining a home made Matlab routine with PIVlab [3]. This allowed us to follow the particles along the flow direction x in the outer part of the rheology cell. A typical example of a measured velocity field is showed in Suppl.Fig. 5c for a correlation window of 0.2 s. In order to obtain the velocity profile on the gap geometry we first spatially averaged the velocity

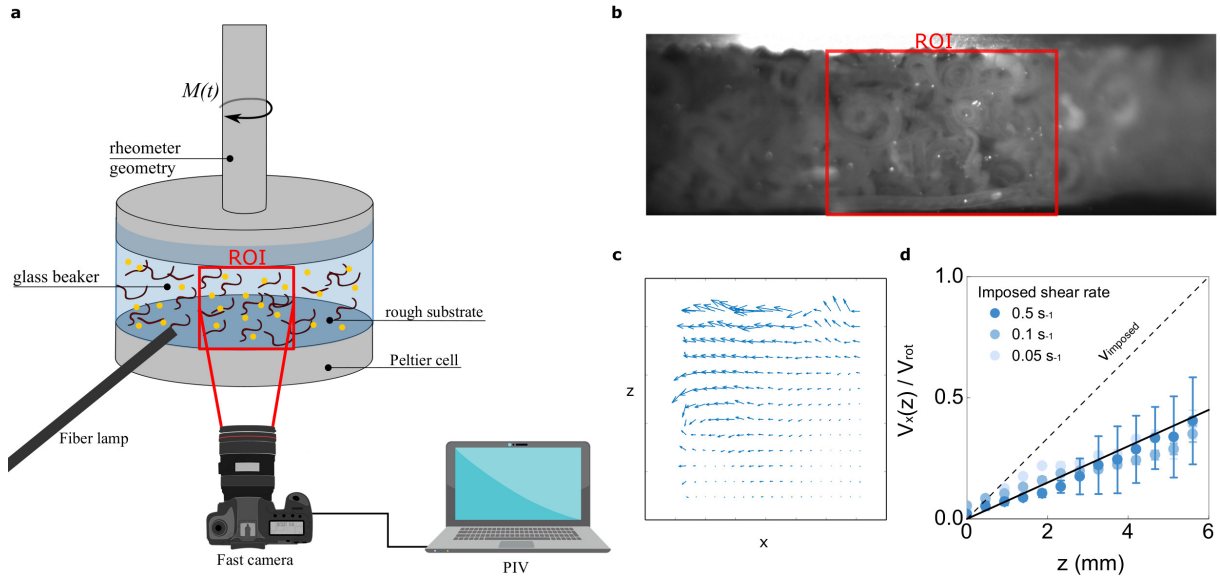

SUPPL. FIG. 5. | **Determination of the velocity profiles from particle image velocimetry (PIV) measurements.** **a** Sketch of the experimental setup used to determine the velocity profiles during the measurements. The active polymer solution is seeded with tracers (hollow silver coated particles d=100μm, LaVision) and tracked in time using a fast camera (Phantom V701).
b View of a typical experiment showing the tracers in reflection light (fiber lamp, Navitar) in the worm solution at a volume fraction of $\phi_{\rm worm} = 0.60$.
c Typical velocity field $V(x, z)$ under the geometry obtained in the region of interest (ROI), highlighted by the red frame in (b). The velocity field is then averaged along the flow direction x and in time (6s) to obtain the velocity profile $V_{\rm x}(z)$ under the geometry shown in (d).
d Averaged velocity profiles for shear rates 0.05, 0.1 and 0.5 $\rm s^{-1}$. The averaged velocity along the flow is normalized by the imposed velocity of the upper geometry $V_{\rm rot}$.

field on the observation window (ROI). Because of the complex consecutive re-arrangements of the worms during their motions inside the geometry, the velocity field can locally exhibit important deviation from a pure shear flow, as vorticity measured from the consecutive velocity fields in time is non-zero (see Suppl.Fig. 5c). We then continued by averaging the obtained velocity profiles in time, chosen as 6 s, the averaged time duration for each point of the rheology measurement. The main results of the the averaged velocity profiles along the geometry gap $V_x(z)$ are shown in Suppl.Fig. 5d. The measurements clearly show for the range of shear rates investigated that the shear rate is all cases overestimated by a factor ~ 2. It appears that in fact, the worms are not entrained in the upper part of the geometry at the desired imposed velocity. For this reason, we corrected all the shear rate values by a factor 2.

3. *Oscillatory measurements*

We performed series of measurement of the storage and loss moduli as function of frequency for a given concentration (1.4 g $\rm cm^{-3}$) of worms in the linear regime ($\gamma = 0.01$). We show on the left graph of Fig. 6 below that, remarkably, $G^{'} \approx G^{''}$ throughout the frequency range f we can span experimentally. This reflects that the *T. tubifex* worms solution is viscoelastic and that the worm entanglements are equally dissipating and storing energy. A further striking feature of the frequency dependence of the shear moduli is that both $G^{'}$ and $G^{''}$ scale with frequency as a power law $G^{'} \approx G^{''} \sim f^{1/2}$. This is very different from what one observes for a material with one single relaxation time due to a combination of factors such as flow-altered intramolecular hydrodynamic interactions and finite extensibility.

We also checked the validity of the Cox-Merz rule:

$$\eta^*(\omega) = \frac{\sqrt{G'^2 + G''^2}}{\omega} \qquad (1)$$

with $\omega = 2\pi f$.

As shown on the right graph of Sup. fig. 6, $\eta(\dot{\gamma}) \approx \eta^*(\omega)$, that is a quite satisfactory agreement for our very complicated system. These measurements invite to further scrutiny and more systematic measurements at different concentrations and level of activity.

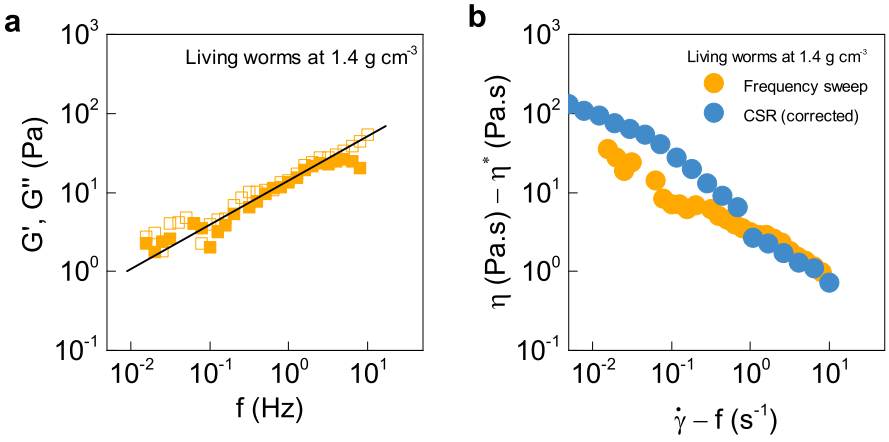

SUPPL. FIG. 6. | **Oscillatory measurements of *T. Tubifex* worm solution.**
a Frequency sweep of the living polymer-like system for a concentration of 1.4 g cm^{-3} and T=20°C. A straight line of slope 1/2 is plotted as a guide for the eye.
b Validity of the Cox-Merz rule. The shear $\eta(\dot{\gamma})$ and the complex viscosity $\eta^*(\omega)$ are plotted as function of the frequency.

[1] M. N. Lazim and M. A. Learner, Ecography **9**, 185 (1986).
[2] J. G. Walker, Biol. Bull. **138**, 235 (1971).
[3] W. Thielicke and E. Stamhuis, Journal of Open Research Software **2**, e30 (2014).